Journal of Applied Nonlinear Dynamics 3(1) (2014) 1–18

Synchronization of coupled map lattice using delayed variable feedback

Siddharth Arora[†], M.S. Santhanam[⋆]

[†]Mathematical Institute, University of Oxford, Woodstock Road, Oxford, OX2 6HD, U.K.

[⋆]Indian Institute of Science Education and Research, Sutarwadi Road, Pashan, Pune, 411 021, India.

Submission Info

Submitted 12 JAN 2014

Keywords

Synchronization 1
Coupled map lattice 2
Multi-channel communications 3

Abstract

We apply the method of variable feedback to obtain complete synchronization in a coupled map lattice. The conditions under which such a synchronization is possible are obtained analytically. We show that synchronization is robust against noise and parameter mismatches. This method leads to synchronized state quite rapidly and we discuss its applications for near-real-time multi-channel communications.

1 Introduction

Synchronization of chaotic systems has received much attention in the last decade since the work of Pecora and Carrol [1]. This has been partly fuelled by potential applications of chaos control, synchronized dynamics in various areas ranging from secure communication, neural networks and pattern formation. Even though, at first sight, it appears that sensitive dependence on initial conditions being the hallmark of chaos might preclude any synchronization from taking place, it has been amply demonstrated that synchronization of chaos is possible [2].

Much of the work on chaos synchronization has focused on low dimensional maps and flows [3] since they form the building blocks for complexity in physical systems. However, many spatio-temporal phenomena in nature are chaotic and at times display synchronization. One of the well known examples is the synchronized neuronal firings recorded by the Electroencephalograph (EEG) devices [4]-[5]. To understand such spatially extended systems coupled map lattice (CML) was introduced by Kaneko [6] as a model for high dimensional chaos capable of displaying a variety of dynamical features including spatio temporal chaos. Recently, the effects of parameter mismatches in synchronized EEG signals and CMLs have been studied extensively [7]. The related question is the synchronization of spatio-temporal chaos in CMLs. The general strategy is to achieve synchronization by an appropriate feedback or drive mechanism. For instance, a generalization of Pecorra and Carrol method suggested by Kocarev and Parlitz, called active passive decomposition has been used to synchronize CMLs [8]. This is based on a general decomposition of any autonomous dynamical system by rewriting it formally as a nonautonomous system with a drive term [8]. In another interesting approach, it was shown that randomly rewiring the CML leads to synchronization [9]. Furthermore, it was demonstrated by Santhanam and Arora [10] that two coupled map lattices that are mutually coupled to one another with a delay can display zero delay synchronization if they are driven by a third coupled map lattice.

In this paper, we obtain complete synchronization in CMLs by applying the continuous feedback technique introduced by Pyragas [11]. Let us suppose that we have two CMLs, named as $X_{n+1}(i)$ and

[†]Corresponding author.
Email address: arora@maths.ox.ac.uk

ISSN 2164 − 6457, eISSN 2164 − 6473/$-see front materials
DOI : 10.5890/JAND.2014.03.001

$Y_{n+1}(i)$, where n and i denote the time and space index respectively. In this method, a suitable form of the signal from X system is fed with a constant delay k at every instant into Y system to finally obtain $X_{n-k}(i) = Y_n(i)$ synchronized state, even when X and Y individually continue to execute chaotic dynamics. This approach was earlier applied to low dimensional maps and flows [12], [13]. We show that the synchronization obtained is robust against noise and parameter mismatches and hence it is useful for practical applications such as the multi-channel communications [14].

Several researchers have investigated the efficacy of chaos synchronization for secure communication [15], [16], [17], [18]. In these applications that require some amount of security, there is a need for as many different chaotic signals as the number of channels to encode the messages sent in each of the channels. Signals sent into these channels are encoded by the chaotic time series from one of the lattice points of the CML. The CML, being a high dimensional chaotic system, is an ideal candidate for such a purpose. Presence of synchronization allows the receiver to decode the message in all the channels. Hence, for real-time applications synchronization must be achieved in shortest possible time. Specifically, the reliability of a chaos-based communication system depends heavily on: a) the robustness of the synchronization scheme to channel noise and potential mismatch in system parameters, and, b) the time it takes to achieve complete chaos synchronization at the receiver and transmitter. In this study, we acheive complete synchronization in CMLs and provide an exhaustive assessment of the robustness of the employed scheme. Based on the reported findings, we argue that the synchronization scheme can be potentially useful for multi-channel secure communication.

2 Complete Synchronization Using Variable Feedback

We consider the CML labelled x given by,

$$x_{n+1}(i) = (1-\epsilon) f[x_n(i)] + \frac{\epsilon}{2}\left(f[x_n(i-1)] + f[x_n(i+1)]\right) \tag{1}$$

where $i = 1, 2....L$ and ϵ is the coupling parameter. We use periodic boundary conditions so that $x_n(L+1) = x_n(1)$ leading to a ring type lattice. The second CML labelled y is obtained by replacing x with y in Eq. (1). Here, the local dynamics uses the logistic equation, $f(x) = ax(1-x)$, where a is the map parameter. The delay feedback technique is implemented by giving a suitable form of $x_{n-k}(i)$ to the y system ($k = 11$ for demonstration). Hence, the modified y-CML becomes,

$$\begin{aligned} y_{n+1}(i) &= (1-\epsilon) f[y_n(i)] + \frac{\epsilon}{2}\left(f[y_n(i-1)] + f[y_n(i+1)]\right) \\ &\quad + H(x_{n-k}, y_n) \end{aligned} \tag{2}$$

where $H(.)$ is the delay feedback term whose specific form we will choose shortly. We are looking for the synchronization state $x_{n-k}(i) = y_n(i)$ and hence we will write the CML dynamics in terms of the variable $z_n(i) = x_{n-k}(i) - y_n(i)$. Using Eqns. (1,2), the dynamics of $z_n(i)$ is given by,

$$\begin{aligned} z_{n+1}(i) &= a(1-\epsilon) z_n(i) + \frac{a\epsilon}{2}\left[z_n(i-1) + z_n(i+1)\right] \\ &- a(1-\epsilon) g_n(i) - \frac{a\epsilon}{2}\left[g_n(i-1) + g_n(i+1)\right] \\ &- H(x_{n-k}, y_n) \end{aligned} \tag{3}$$

where $g_n(i) = x^2_{n-k}(i) - y^2_n(i)$. The target synchronization state is $z_n(i) = 0$, for $i = 1, 2...L$. Now, we will choose

$$\begin{aligned} H &= (1-\epsilon)\left[(a-\rho) z_n(i) - a g_n(i)\right] \\ &+ \frac{\epsilon}{2}\left[(a-\rho) z_n(i+1) - a g_n(i+1)\right. \\ &+ \left.(a-\rho) z_n(i-1) - a g_n(i-1)\right] \end{aligned} \tag{4}$$

such that it would serve to cancel $g_n(.)$ and $z_n(.)$ in Eq. (3) and introduce ρ as a parameter to control the strength of the feedback. The general strategy is to choose a H so that all except the terms linear in ρz_n are canceled. Earlier, this has been adapted to synchronize a logistic map [12]. While this is one simple choice for H, this is not unique. Some of the properties discussed later depend on this particular strategy for choosing H. Now, substituting H in Eq. (3), we can write down the resulting equation in matrix form as $Z_{n+1} = \mathbf{A}Z_n$, where $Z_n = \{z_n(1), z_n(2), ...z_n(L)\}^T$ is the column vector and $\mathbf{A}$ is the Jacobian matrix given by,

$$\mathbf{A} = \begin{pmatrix} a_1 & a_2 & 0 & ... & a_L \\ a_L & a_1 & a_2 & ... & 0 \\ \vdots & \vdots & \vdots & \vdots & \vdots \\ a_L & 0 & ... & ... & a_1 \end{pmatrix}$$

with $a_1 = \rho(1-\epsilon)$ and $a_2 = a_L = \rho\epsilon/2$. The eigenvalues of $\mathbf{A}$ are

$$\begin{aligned} \lambda_{k_1} &= \sum_{j=1}^{L} a_j \; e^{i2\pi k_1 j/L} \qquad k_1 = 1, 2, ..L. \\ &= e^{i2\pi k_1/L} \, [a_1 + 2a_2 \cos(2\pi k_1/L)] \end{aligned} \tag{5}$$

A homogeneous synchronization state requires $\mid \lambda_{k_1} \mid < 1$ for all k_1. It is straightforward to show that this requirement is equivalent to,

$$\rho < 1, \quad \text{and} \quad \epsilon < (1/2)[1 + (1/\rho)]. \tag{6}$$

As $n \to \infty$, $z_{n+1}(i) = x_{n-k+1}(i) - y_{n+1}(i) \to 0$ and systems (1) and (2) are perfectly synchronized. Notice that this is also the condition for stable synchronized state and hence $\rho < 1$ also ensures the stability of the synchronized state. The conditions in Eq. (6) are independent of the map parameter a and for $\rho < 1$, we have $\epsilon < 1$.

We show the results of numerical simulations for CMLs given by Eqns (1,2) with periodic boundary conditions and starting from different random initial conditions. The parameters used are $\rho = 0.1$ with $a = 4.0$ and $\epsilon = 0.9$ corresponding to spatio-temporal chaos [19] and satisfy the requirements for synchronization. In Fig 1(a,b) we show the CML output drawn from 56th lattice. Except for the first few iterations, both display similar dynamics. The error $z_n(i) = x_{n-k}(i) - y_n(i)$ shown in Fig 1(c), is of $O(10^{-5})$ after a few iterations and provides an evidence of synchronization, which is achieved in about 4 iterations. In Fig 2, we show $z_n(i)$ as a space-time plot. Clearly, all the 100 lattices synchronize very quickly and remain so as $n \to \infty$.

3 Robustness of the scheme

We check the robustness of the proposed scheme with respect to additive noise and parameter mismatch. In the presence of noise, the CML in Eqns (1,2) is modified as,

$$\begin{aligned} x_{n+1}(i) &= F(x_n) + \nu_n(i) \\ y_{n+1}(i) &= G(x_{n-k}, y_n) + \mu_n(i) \end{aligned} \tag{7}$$

where F and G represent the right hand side of Eqns (1) and (2) respectively. The noise terms $\nu_n(.)$ and $\mu_n(.)$ are uniformly distributed random numbers in the range [0,0.01]. If $\nu_{n-k}(i) = \mu_n(i)$, then the noise in one CML will be canceled by the other and the results discussed above hold without any change. If $\nu_{n-k}(i) \neq \mu_n(i)$, then the synchronization persists though with a bounded error. This result can be obtained as follows. We denote a column vector of noise by $\Gamma_n = \{\nu_{n-k}(1) - \mu_n(1), \nu_{n-k}(2) -$

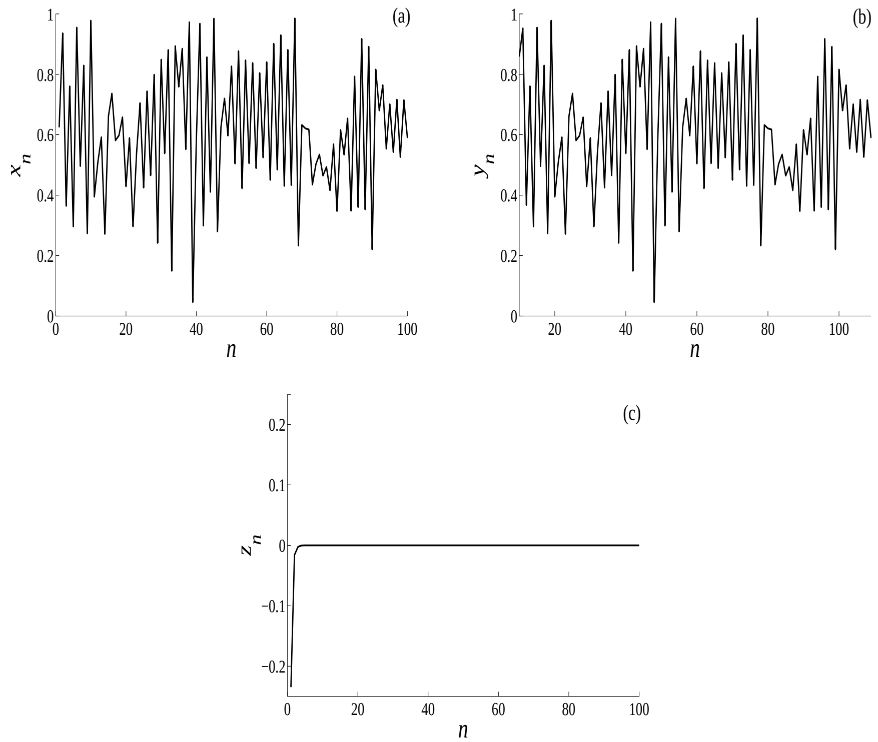

Fig. 1: Temporal evolution of the CML for 56th lattice point. (a) $x_n(56)$, (b) $y_n(56)$, (c) $z_n(56)$.

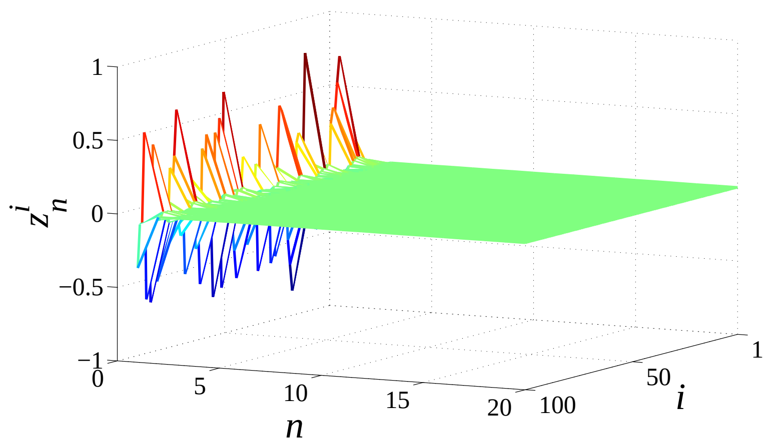

Fig. 2: Error $z_n(i)$ for $L = 100$ lattice points iterated for 20 time steps. Note that synchronization is marked by the flat plane at about $z_n(i) = 0.0$.

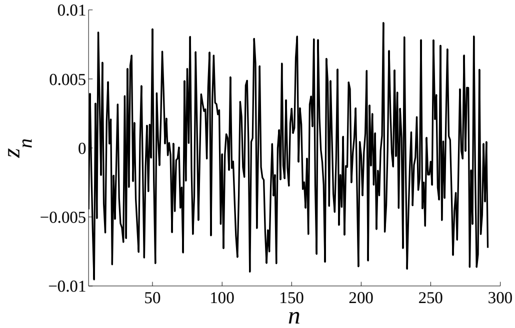

Fig. 3: Error due to the presence of additive noise for the 56th lattice of CML in Eqns (1,2).

$\mu_n(2), ...\nu_{n-k}(L)-\mu_n(L)\}^T$. In the presence of noise, the error dynamics is given by $Z_{n+1} = \mathbf{A}Z_n+\Gamma_n$. If $\mathbf{R}$ is the matrix that diagonalizes $\mathbf{A}$ such that $\mathbf{RAR^{-1}} = \mathbf{\Lambda}$, where $\mathbf{\Lambda} = \text{diag}\{\lambda_1, \lambda_2, ...\lambda_L\}$ is a diagonal matrix. Now, using the shorthand notation $Z_n^{'} = \mathbf{R}Z_n$ and $\Gamma_n^{'} = \mathbf{R}\Gamma_n$, we get, $Z_{n+1}^{'} = \mathbf{\Lambda}Z_n^{'} + \Gamma_n^{'}$. In scalar form, this equation becomes,

$$\begin{aligned} z_n^{'}(i) &= \lambda_i \, z_{n-1}^{'}(i) + (\nu_{n-k-1,l}^{'} - \mu_{n-1,l}^{'})(i) \\ &= \lambda_i^n \, z_0^{'}(i) + (\nu_{n-k,l}^{'} - \mu_{n,l}^{'})(i), \end{aligned} \tag{8}$$

where μ' and ν' are the noise terms transformed by $\mathbf{R}$. The second form of Eq. (8) is obtained by starting from an initial $z_0^{'}(i)$ and iterating n times. From this, we obtain the following inequality,

$$z_n^{'}(i) \leqslant \lambda_i^n |z_0^{'}(i)| + \phi_i \sum_{j=0}^{n-1} \lambda_i^j = \lambda_i^n |z_0(i)| + \frac{\phi_i}{1-\lambda_i} \tag{9}$$

where $\phi_i = \max(\nu_{n-k,l}^{'} - \mu_{n,l}^{'})(i)$ is bounded and so is the error due to addition of noise. Fig 3 shows that the error due to additive noise is of $O(10^{-3})$. In Eq. (9), $\lambda_i^n \to 0$ as $n \to \infty$. In our numerics, $\phi_i \sim O(10^{-3})$ and $\lambda_i < 1$. As shown in Fig 3, the error is well within the estimated bounds. It remains so for all the lattice points.

When the coupling parameters of the two systems are slightly mismatched, synchronization is still realized though with some error. The basic CML labelled x is given by Eq. (1) and the y-system is,

$$\begin{aligned} y_{n+1}(i) &= (1-\bar{\epsilon})f[y_n(i)] + \frac{\bar{\epsilon}}{2}\left(f[y_n(i-1)] + f[y_n(i+1)]\right) \\ &\quad +H(x_{n-k}(i), y_n(i)) \end{aligned} \tag{10}$$

The error $\hat{z}$ for a mismatch $\Delta\epsilon = \epsilon - \tilde{\epsilon}$ is,

$$\hat{z}_{n+1}(i) = z_{n+1}(i) - \frac{\Delta\epsilon}{2}\,\mathcal{F}(x_{n-k}) \tag{11}$$

where $z_n(.)$ is defined in Eq. (3) and $\mathcal{F}(x_{n-k}) = 2f[x_{n-k}(i)] - f[x_{n-k}(i+1)] - f[x_{n-k}(i-1)]$. It can be shown that $\hat{z}$ will remain bounded if $\mathcal{F}(x_{n-k}) < x_{max}$. This implies that if the condition $|\ \Delta\epsilon\ x_{max}/2\ | \ll 1$ is satisfied, synchronization will be achieved but will suffer a small but bounded error of $O(|\Delta\epsilon\ x_{max}/2|)$. In Fig 4, we show the simulation result for the 56th lattice of systems in Eq. (1,10). We have $\Delta\epsilon/2 = 0.005$ corresponding to $\epsilon = 0.9$ and $\bar{\epsilon} = 0.89$. Since typically $x_{max} \sim O(1)$, the estimated error in this case is $O(10^{-3})$ which is borne out by the numerical results in the Fig 4. Even though, we have not shown here, this result holds true for all the lattice sites in the CML.

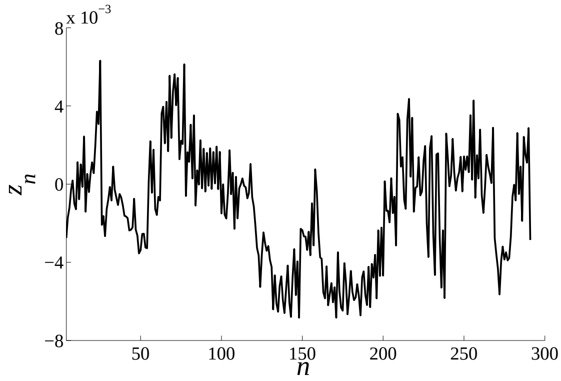

Fig. 4: Error $\hat{z}$ due to parameter mismatch shown for a typical lattice $(i = 56)$ for $\epsilon = 0.9$, $\bar{\epsilon} = 0.89$.

Next, we consider the mismatch in the map parameter a. Once again, Eq. (1) represents the x-system and Eq. (2) is the y-system with its a replaced by $\tilde{a}$. In this case, the dynamics of error $\hat{z}$ becomes,

$$\begin{aligned}\hat{z}_{n+1}(i) &= z_{n+1}(i) + \frac{(a-\tilde{a})}{a}\left\{(1-\epsilon)f[x_{n-k}(i)]\right.\\ &\left.+\frac{\epsilon}{2}\left(f[x_{n-k}(i-1)] + f[x_{n-k}(i+1)]\right)\right\}\end{aligned} \tag{12}$$

Note that after synchronization is achieved, $z_{n+1}(i) = 0$ and Eq. (12) is simply the CML equation scaled by the factor $\Delta a = (1 - \tilde{a}/a)$. Hence, the error due to mismatch in the local map parameter a can be made arbitrarily small by tuning Δa. In Fig 5, we show CMLs evolved under a mismatch in map parameter; i.e, we take $a = 4, \tilde{a} = 3.99$ such that $\Delta a = 0.0025$. The solid line in the figure corresponds to $\hat{z}_n(56)$ and the dashed line to $\Delta a\ x_{n-k}(56)$, i.e, the output of 56th lattice $x_n(56)$ scaled by Δa. Except for first few iterations, both the curves coincide to within the numerical errors thus confirming Eq. (12). Hence, this synchronization scheme is robust against noise and parameter mismatches. Both these properties are important for devising practical applications based on this scheme. Our results show that the synchronization discussed here is independent of the system size, i.e, all the properties discussed above and time T_{sync} taken to achieve synchronization (defined as the number of iterations needed at which $z(i) < 10^{-5}$) are the same irrespective of number of lattice points in the CML. Physically, this is to be expected since every lattice point is connected to its nearest neighbors and each of them see the same environment. Hence the properties of all the lattice points are the same.

We investigate if the x and y CMLs are phase synchronized. The phenomenon of phase synchronization has been extensively studied by many researchers [20], [21]. In Fig 6, we plot the phase of the 56th lattice of x and y CMLs, as specified in Eq. (1, 2). As evident from Fig 6, the x and y-system lattices are phase synchronized.

As pointed out earlier, time to achieve synchronization is $T_{sync} \sim 4$ iterations and is the same for any number of lattice points in the CML but it does vary with the parameter ρ that controls the strength of feedback. Fig 7 shows that as $\rho \to 1$, the synchronization time increases monotonically. This is an indication that for $\rho > 1$, synchronization is not possible. This, in turn, is in agreement with the Eq. (6) derived earlier.

This scheme is reasonably robust to noise implying that the noise due to electronic circuits will not spoil the synchronization features. Similar robustness holds good for small mismatches in circuit parameters that are required to build electronic equivalents of CMLs. In particular, time to synchronize is quite short. The properties discussed above lends the scheme to be useful for secure, real-time multi-channel communication. Another possible extension of this is to choose H such that noise in one

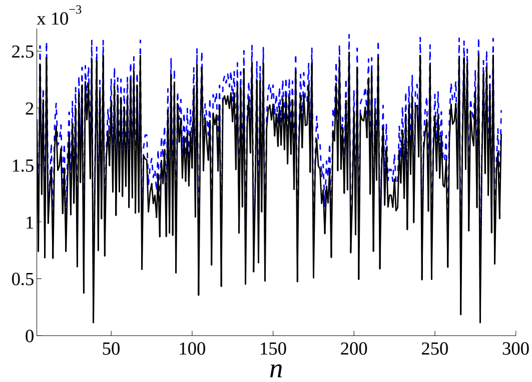

Fig. 5: Error $\hat{z}$ due to parameter mismatch shown for a typical lattice ($i = 56$) for $a = 4$, $\tilde{a} = 3.99$; The black curve is the CML output in Eq. (1) scaled by Δa.

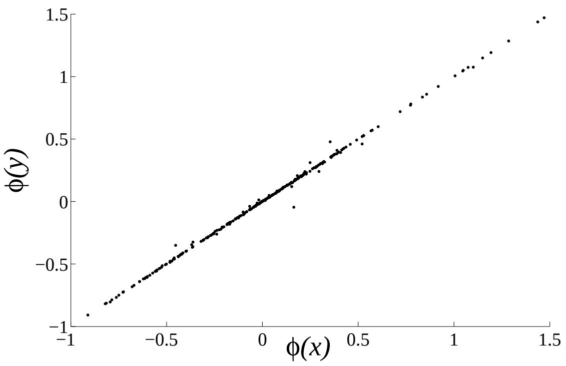

Fig. 6: Phase of a typical lattice (i=56) belonging the x and y-systems, denoted by $\phi(x)$ and $\phi(y)$, respectively.

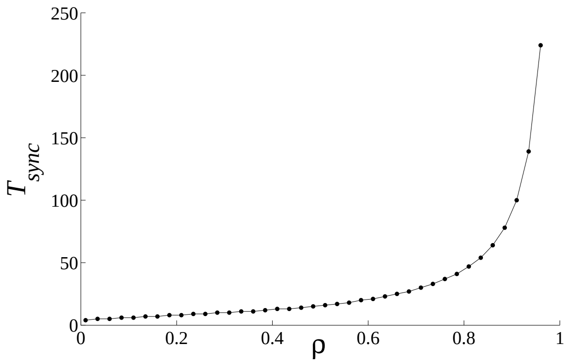

Fig. 7: Time taken to synchronize all the lattice points, i.e, number of iterations (T_{sync}) as a function of ρ that controls the strength of feedback.

channel is not propogated into any other channel. Further, this scheme can be adopted for any local map $x_{n+1} = f(x_n)$ other than logistic map. Then, the quantitative details of the results may be different from that presented here for the case of logistic map. Further, one could consider other types of CMLs such as the one-way coupled lattices with periodic boundary conditions. We find that qualitatively we obtain similar results as discussed above. This method can also be extended to synchronize two dimensional coupled map lattices.

4 Conclusions

In this study, we showed that the complete synchronization of coupled map lattices can be achieved by applying the method of variable feedback. We analytically obtained the conditions on the parameters that will lead to synchronization. Furthermore, we demonstrated that this synchronization scheme is quite fast and is robust against noise and parameter mismatches. This is a crucial feature for practical applications like near-real-time secure multichannel communications.

References

[1] Pecora, L.M. and Carroll, T.L. (1990), Synchronization in chaotic systems, *Physical Review Letters*, **64**, 821-825.
[2] Pikovsky, A., Rosenblum, M. and Kurths, J. (2001), *Synchronization: A universal concept in nonlinear sciences*, (Cambridge).
[3] Boccaletti; S., Kurths, J., Osipov, G., Valladares, D.L. and Zhou, C.S. (2002), The synchronization of chaotic systems, *Physics Reports*, **366**, 1-101.
[4] Glass, L. (2001), Synchronization and rhythmic processes in physiology, *Nature*, **410**, 277-284.
[5] Quian Quiroga, R., Kraskov, A., Kreuz, T. and Grassberger, P. (2002), Performance of different synchronization measures in real data: A case study on electroencephalographic signals, *Physical Review E*, **65**, 041903-14.
[6] *Theory and applications of coupled map lattices*, edited by K. Kaneko (Wiley, New York, 1993).
[7] Ahalpara, D.P., Arora, S. and Santhanam, M.S. (2009), Genetic programming based approach for synchronization with parameter mismatches in EEG, *Lecture Notes in Computer Science*, **5481**, 13-24.
[8] Kocarev, L. and Parlitz, U. (1995), General approach for chaotic synchronization with applications to communication, *Physical Review Letters*, **74**, 5028-5031; Jinlan, W., Guangzhi, C., Tuanfa, Q., Wansun, N. and Xuming, W. (1998), Synchronizing spatiotemporal chaos in coupled map lattices via active-passive decomposition, *Physical Review E*, **58**, 3017-3021.
[9] Sinha, S. (2002), Random coupling of chaotic maps leads to spatiotemporal synchronization, *Physical Review E*, **66**, 016209-6.
[10] Santhanam, M.S. and Arora, S. (2007), Zero delay synchronization of chaos in coupled map lattices, *Physical Review E*, **76**, 026202-8.
[11] Pyragas, K. (1992), Continuous control of chaos by self-controlling feedback, *Physics Letters A*, **170**, 421-428.
[12] Morgul, O. (1998), On the synchronization of logistic maps, *Physics Letters A*, **247**, 391-396.
[13] Ali, M.K. and Fang, J-Q. (1997), Synchronization of chaos and hyperchaos using linear and nonlinear feedback functions, *Physical Review E*, **55**, 5285-5290.
[14] Xiao, J.H., Hu, G. and Qu, Z. (1996), Synchronization of Spatiotemporal Chaos and Its Application to Multichannel Spread-Spectrum Communication, *Physical Review Letters*, **77**, 4162-4165.
[15] Argyris, A., Syvridis, D., Larger, L., Annovazzi-Lodi, V., Colet, P., Fischer, I., Garcia-Ojalvo, J., Mirasso, C.R., Pesquera, L. and Shore, K.A. (2005), Chaos-based communications at high bit rates using commercial fibre-optic links, *Nature*, **438**, 343-346.
[16] Moskalenko, O.I., Koronovskii, A.A. and Hramov, A.E. (2010), Generalized synchronization of chaos for secure communication: Remarkable stability to noise, *Physics Letters A*, **374**, 2925-2931.
[17] Kinzel, W., Englert, A. and Kanter, I. (2010), On chaos synchronization and secure communication, *Philosophical Transactions of the Royal Society: A*, **368**, 379-389.
[18] Li, P., Wu, J-G., Wu, Z-M., Lin, X-D., Deng, D., Liu, Y-R. and Xia, G-Q. (2011), Bidirectional chaos communication between two outer semiconductor lasers coupled mutually with a central semiconductor laser, *Optics Express*, **19**, 23921-23931.

[19] Kaneko, K. (1989), Spatiotemporal chaos in one- and two-dimensional coupled map lattices, *Physica D*, **37**, 60-82.

[20] Pikovsky, A.S., Rosenblum, M.G., Osipov, G.V. and Kurths, J. (1997), Phase synchronization of chaotic oscillators by external driving, *Physica D: Nonlinear Phenenomena*, **104**, 219-238.

[21] Shabunin, A., Demidov, V., Astakhov, V. and Anishchenko, V. (2002), Information theoretic approach to quantify complete and phase synchronization of chaos, *Physical Review E*, **65**, 056215-5.